

Blueshift in $\text{Mg}_x\text{Zn}_{1-x}\text{O}$ alloys: Nature of bandgap bowing

Almamun Ashrafi^{1(a)} and Yusaburo Segawa²

¹Department of Electronic Materials Engineering, Research School of Physical Sciences and Engineering, The Australian National University, Canberra 0200, Australia

²Frontier Research System, Institute of Physical and Chemical Research, Wako 351-0198, Japan

(Received 30 July 2008; accepted 7 November 2008; published online 23 December 2008)

A Mg composition-dependent blueshift has been studied in $\text{Mg}_x\text{Zn}_{1-x}\text{O}$ alloys deposited on 6H-SiC(0001) substrates. The localized exciton energy in $\text{Mg}_x\text{Zn}_{1-x}\text{O}$ alloys for $x \sim 0.3$ was blueshifted in the range 212–248 meV. The large negative bowing parameter was estimated in $\text{Mg}_x\text{Zn}_{1-x}\text{O}$ alloys to be 4.72 ± 0.84 eV. This large bandgap bowing emphasizes the Stokes shift, which has been attributed to the existence of spontaneous polarization effects due to the polar growth of $\text{Mg}_x\text{Zn}_{1-x}\text{O}/\text{SiC}$ heterostructure and local compositional inhomogeneity. © 2008 American Institute of Physics. [DOI: 10.1063/1.3050338]

I. INTRODUCTION

Wurtzite (Mg, Zn, Be, Cd)O materials provide enormous practical benefits as promising candidates for the use of exciton-based laser diodes, light emitting diodes, and optical sensors/detectors operating in the visible to ultraviolet spectral regions due to their large bandgap energy covering from 2.24 to 7.60 eV.^{1,2} Experimental and theoretical studies have extensively been addressed to the extraordinary optical and transport properties of (Mg, Zn, Cd)O materials relevant to such applications.^{1,2} However, practical applications and studies of (Mg, Zn, Cd)O materials system are still a challenge, since the shallow thermodynamic solubility and disorder of atoms locally play a significant role in the (Mg, Zn, Cd)O matrix. In consequence, the $\text{Mg}_x\text{Zn}_{1-x}\text{O}$ heterostructure alloying is still immature and requires exclusive studies especially to clarify the solubility limit and the microscopic character of Mg atoms. The thermodynamic shallow solubility limit of Mg in ZnO has been reported of 12%,³ primarily due to their structural dissimilarities as the ZnO and MgO materials are stable with wurtzite and rocksalt phases, respectively. This structural mismatch causes phase segregation triggered by the strain kinetics and finally limits the Mg incorporation into the ZnO matrix.¹⁻³ A strong variation with Mg composition has been found for the fundamental energy gap of the $\text{Mg}_x\text{Zn}_{1-x}\text{O}$ alloys.⁴ It has been expected that this is accompanied by a bandgap bowing and giant energy shift between the photoluminescence (PL) peaks and absorption edges, so-called Stokes shift. In addition, the microscopic polarization in the $\text{Mg}_x\text{Zn}_{1-x}\text{O}/\text{Al}_2\text{O}_3$ heterointerface has a major influence on the design criteria of alloys that impact significantly to the optical and transport properties.³ Therefore, these complex limitations play the crucial roles in heteroepitaxy and degrade the crystalline quality.

Wurtzite ZnO has a direct bandgap energy of 3.37 eV,^{1,2} corresponding to the near ultraviolet region of the spectrum. This bandgap energy can further be raised into the ultraviolet region by alloying with MgO ($E_g \sim 5.20$ eV) or lowered into the visible/blue region by alloying with CdO material (E_g

~ 2.24 eV).² To a first approximation, the bandgap energy engineering of any alloy, such as $\text{Mg}_x\text{Zn}_{1-x}\text{O}$, can be tailored using the composition-weighted average of ZnO and MgO bandgaps, given by $E_{\text{Mg}_x\text{Zn}_{1-x}\text{O}}(x) = xE_{\text{MgO}} + (1-x)E_{\text{ZnO}}$. A more realistic description includes a nonlinear term given by $E_{\text{Mg}_x\text{Zn}_{1-x}\text{O}}(x) = xE_{\text{MgO}} + (1-x)E_{\text{ZnO}} - \delta x(1-x)$, known as Vegard's law, where δ is known as the bandgap bowing parameter and x is the Mg composition. Recently, our group has reported a routine determination of Mg composition in the $\text{Mg}_x\text{Zn}_{1-x}\text{O}$ alloys by employing Vegard's law and a theoretical model within an error limit of $\sim 3\%$.⁴ In addition, it has been demonstrated that PL peak energies of $\text{Mg}_x\text{Zn}_{1-x}\text{O}$ alloys do not comply with the conventional (downward parabolic) Vegard's law.⁴ In principle, parabolic (upward or downward) compositional dependence is assumed for the bandgap of alloys, where δ captures the magnitude of parabolic nonlinearity.⁵ To get a clear picture on this upward parabolic nature in $\text{Mg}_x\text{Zn}_{1-x}\text{O}$ alloys deposited on SiC substrates, PL, absorption (AB), reflectance (RF), and x-ray diffraction (XRD) measurements were performed. The localized exciton energy (E_{ex}) of $\text{Mg}_x\text{Zn}_{1-x}\text{O}$ alloys for $x \sim 0.30$ is blueshifted in the range 212–248 meV. A large bandgap bowing of -4.72 eV in the $\text{Mg}_x\text{Zn}_{1-x}\text{O}$ alloys emphasizes the large Stokes shift, which has been attributed to the spontaneous polarization experienced in the heterointerfaces and compositional disorder of Mg atoms locally.

II. EXPERIMENT

$\text{Mg}_x\text{Zn}_{1-x}\text{O}$ alloys were grown on 6H-SiC(0001) substrates by metalorganic chemical-vapor deposition. The substrate cleaning and processing have been described in detail elsewhere.^{4,6} The $\text{Mg}_x\text{Zn}_{1-x}\text{O}$ alloys were deposited at the atmospheric pressure over the selected substrate temperature (T_g) range of 400–600 °C. Diethyl zinc (DEZn) and bis-methyl cyclopentadienyl-magnesium [(MeCp)₂Mg] were allowed to flow for ~ 20 s prior to the introduction of O₂. During the deposition of $\text{Mg}_x\text{Zn}_{1-x}\text{O}$ alloys, the flow rates of (MeCp)₂Mg and O₂ were kept constant at 20 and 10 SCCM (SCCM denotes cubic centimeter per minute at STP), respectively, while the flow rate of DEZn was varied from 0 to 12

^aElectronic mail: ash2phy@yahoo.com.

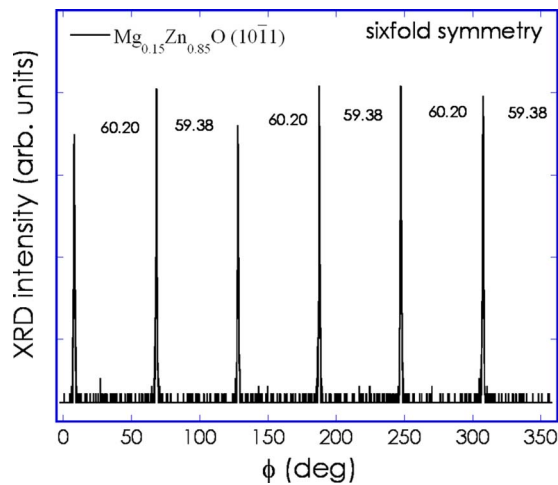


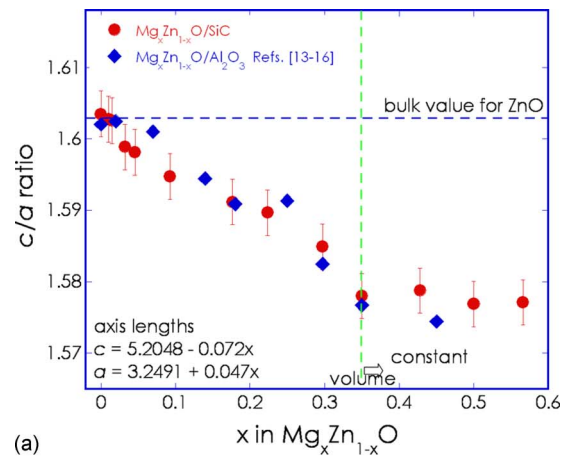
FIG. 1. (Color online) The ϕ -scan of $\text{Mg}_{0.15}\text{Zn}_{0.85}\text{O}\{10\bar{1}1\}$ alloy deposited on $\text{SiC}(0001)$ substrate, indicating the sixfold symmetry with polar growth along the c axis. The typical $\text{Mg}_x\text{Zn}_{1-x}\text{O}$ layer thickness was $0.75 \mu\text{m}$.

SCCM. The $\text{Mg}_x\text{Zn}_{1-x}\text{O}$ alloys have been characterized by ϕ scan using the four-circle diffractometer: XRD, PL, RF, and AB measurements.⁷ The typical $\text{Mg}_x\text{Zn}_{1-x}\text{O}$ layer thickness was $0.75 \mu\text{m}$. Calculation of Zn and Mg composition in the $\text{Mg}_x\text{Zn}_{1-x}\text{O}$ alloys has been reported in Ref. 4.

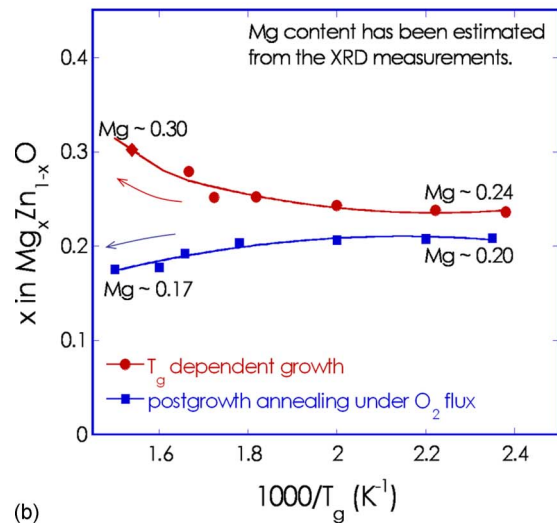
III. RESULTS AND DISCUSSION

Figure 1 shows the ϕ scan of $\text{Mg}_{0.15}\text{Zn}_{0.85}\text{O}\{10\bar{1}1\}$ planes, which clearly display a sixfold crystal symmetry. This observation conclusively reveals a hexagonal structure of $\text{Mg}_x\text{Zn}_{1-x}\text{O}$ alloys grown on SiC substrates. An epitaxial relationship in the $\text{Mg}_x\text{Zn}_{1-x}\text{O}/\text{SiC}$ heterostructures was found to be $(11\bar{2}0)_{\text{Mg}_x\text{Zn}_{1-x}\text{O}} \parallel (11\bar{2}0)_{\text{SiC}}$ and $(0001)_{\text{Mg}_x\text{Zn}_{1-x}\text{O}} \parallel (0001)_{\text{SiC}}$. These results obviously indicate the polar growth, i.e., the $\text{Mg}_x\text{Zn}_{1-x}\text{O}$ alloys grow along the c axis. The calculated lattice constants of a and c axis lengths of $\text{Mg}_x\text{Zn}_{1-x}\text{O}$ alloys by the c/a ratio as a function of Mg content have been plotted in Fig. 2(a). For comparison, the c/a ratio of $\text{Mg}_x\text{Zn}_{1-x}\text{O}$ alloys grown on Al_2O_3 substrates has been plotted together with those of the $\text{Mg}_x\text{Zn}_{1-x}\text{O}/\text{SiC}$ heterostructure, cited from Ref. 8. This shows that the c/a ratio decreases monotonically from 1.602 to 1.575 until the Mg composition reaches 34% with the increase in Mg content in both the heterostructures. This observation clearly indicates that the c/a ratio does not decrease further since the cell volume reaches a constant value. In principle, incorporation of Mg into the wurtzite ZnO structure expands the unit cell resulting in a total volume expansion. These results suggest that the phase segregation may about to start in the $\text{Mg}_x\text{Zn}_{1-x}\text{O}$ alloys for $x \geq 34\%$, which agrees well with the $\text{Mg}_x\text{Zn}_{1-x}\text{O}/\text{Al}_2\text{O}_3$ heterostructure.^{4,6,8} Therefore, we will deal the blueshift and bandgap bowing in $\text{Mg}_x\text{Zn}_{1-x}\text{O}$ alloys for the Mg composition of $x < 34\%$.

The thermodynamic instability/stability of Mg content in the $\text{Mg}_x\text{Zn}_{1-x}\text{O}$ alloys has been studied by T_g dependence growth and the subsequent postgrowth annealing. For the T_g dependent $\text{Mg}_x\text{Zn}_{1-x}\text{O}$ alloys, Mg flow rate was kept constant for 20 SCCM. Figure 2(b) shows that with the increase in T_g , Mg content increases due to the relatively faster de-



(a)



(b)

FIG. 2. (Color online) The (a) c/a ratio and (b) deposition and postgrowth annealing temperature-dependent (T_g) $\text{Mg}_x\text{Zn}_{1-x}\text{O}$ alloys as a function of Mg composition. The postgrowth annealing was done for 30 min under the O_2 flux at the atmospheric pressure.

crease in sticking coefficient of Zn species, due to their different vapor pressures. It has been reported that the vapor pressure of Zn species is higher than that of the Mg ($\text{Zn} > \text{Mg}$),⁸ suggesting that Zn might preferentially desorb from the growing surface, leaving the Mg-rich solid phase. To explore this character, postgrown $\text{Mg}_x\text{Zn}_{1-x}\text{O}$ alloys were annealed at different temperatures inside a furnace under the O_2 ambient. Figure 2(b) shows that with the increase in annealing temperature for $\text{Mg}_x\text{Zn}_{1-x}\text{O}$ alloys, the Mg content decreases, clearly contradicting with the suggested T_g -dependent growth. As the postgrowth annealing was done under the atmospheric pressure, it is expected that even under the O_2 ambient, the $\text{Mg}_x\text{Zn}_{1-x}\text{O}$ alloys may be with the Zn-rich rather than the Mg-rich conditions. It is true that under the same growth conditions, growth rate of ZnO epilayer is faster than that of the MgO thin films. However, to clarify this thermal behavior and control the solid composition in $\text{Mg}_x\text{Zn}_{1-x}\text{O}$ alloys under the postgrowth annealing, further investigations are necessary.

Figure 3(a) shows the optical responses of ZnO epilayers at 3.301, 3.332, and 3.331 eV in the PL, RF, and AB spectra, respectively. The PL spectrum of ZnO epilayers exhibited a

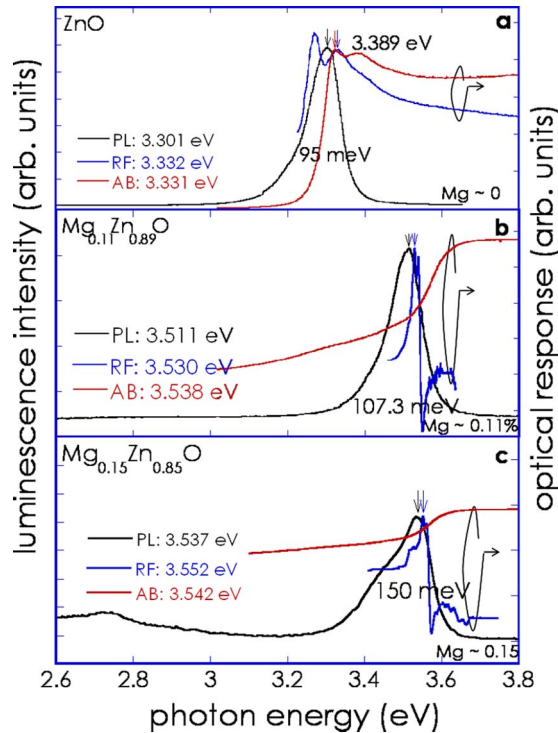


FIG. 3. (Color online) Optical properties of (a) ZnO, (b) $\text{Mg}_{0.11}\text{Zn}_{0.89}\text{O}$, and (c) $\text{Mg}_{0.15}\text{Zn}_{0.85}\text{O}$ layers studied by PL, RF, and AB measurements. The full width at half maximum of the respective epilayers has been marked, which clearly increases with the increase in Mg content in the $\text{Mg}_x\text{Zn}_{1-x}\text{O}$ alloys.

predominant near bandedge emission at 3.30 eV. The PL peak is assigned as being due to the recombination of excitons bound to certain impurities or defects.^{1,4} The A-exciton transition is clearly observed in the RF and AB spectra (3.331 eV), with the B-exciton peak (3.389 eV) visible at room temperature. Figures 3(b) and 3(c) show the systematic Mg composition-dependent optical properties of $\text{Mg}_x\text{Zn}_{1-x}\text{O}$ layers deposited on SiC. Throughout the experiments, the E_{ex} of $\text{Mg}_x\text{Zn}_{1-x}\text{O}$ alloys were dominant in the optical spectra. The PL spectra of $\text{Mg}_{0.11}\text{Zn}_{0.89}\text{O}$ and $\text{Mg}_{0.15}\text{Zn}_{0.85}\text{O}$ alloys exhibited predominantly the E_{ex} emissions at 3.511 and 3.537 eV, respectively. The absorption edges of the $\text{Mg}_{0.11}\text{Zn}_{0.89}\text{O}$ and $\text{Mg}_{0.15}\text{Zn}_{0.85}\text{O}$ layers were recorded to be 3.538 and 3.542 eV, while the excitonic transitions in the RF spectra were 3.530 and 3.552 eV, respectively. The E_{ex} values obtained for the $\text{Mg}_x\text{Zn}_{1-x}\text{O}$ epilayers (3.30–3.54 eV for $x=0-0.20$) are larger than that of the binary ZnO layers, and are comparable to that reported for the $\text{Mg}_x\text{Zn}_{1-x}\text{O}$ alloys deposited on Al_2O_3 substrates.^{4,8} Although there are some energy differences among the PL, RF, and AB spectra, these results are broadly indicative of the compositional inhomogeneity, generally referred to as the Stokes shift.

Figure 4 shows the experimental E_{ex} and Stokes shift of $\text{Mg}_x\text{Zn}_{1-x}\text{O}$ alloys as a function of Mg content. The E_{ex} increases with the increase in Mg content in $\text{Mg}_x\text{Zn}_{1-x}\text{O}$ alloys for $x \leq 0.2$ by 212–248 meV. However, the rate of change of E_{ex} in the $\text{Mg}_x\text{Zn}_{1-x}\text{O}$ layers due to Mg composition is different from the III-N materials.⁹ The III-N alloys follow the downward parabola, while the $\text{Mg}_x\text{Zn}_{1-x}\text{O}$ alloy follows the upward parabola of Vegard's law. The E_{ex} increases with the upward bowing in the $\text{Mg}_x\text{Zn}_{1-x}\text{O}$ layers similarly to the

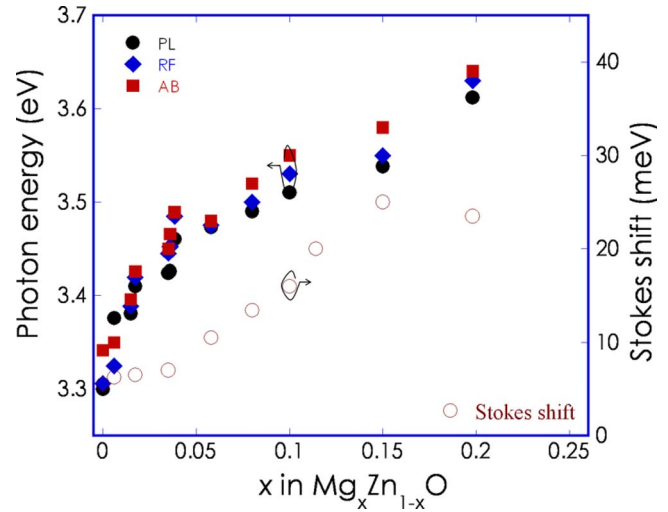


FIG. 4. (Color online) The PL (●), RF (◆), and AB (■) energies and Stokes shift (○) in $\text{Mg}_x\text{Zn}_{1-x}\text{O}$ alloys as a function of Mg composition.

other results demonstrated in the $\text{Mg}_x\text{Zn}_{1-x}\text{O}$ alloys.^{1,2,4-6} In principle, the negative bowing parameter emphasizes an upward bowing due to defects or impurities and/or compositional inhomogeneity in the (Mg, Zn)O matrix. These parameters emphasize the large Stokes shift that has been recorded to be ~ 30 meV in the optical bands as shown in Fig. 4.

Although an upward bandgap bowing tendency of the E_{ex} in $\text{Mg}_x\text{Zn}_{1-x}\text{O}$ alloys was obtained, there is no experimental evidence of this bowing parameter, δ , in literature. In this work, we have estimated δ by a different approach than the conventional Vegard's law.¹⁰ It has been demonstrated that regardless of the alloy structure and composition, the spontaneous polarization always shows an upward bowing.¹¹ In this context, the accuracy of δ is limited by two main factors: composition and PL energy position fluctuations at room temperature. We assume that both of these factors have the same influence on the experimental accuracy. The compositional inhomogeneity, Δx , can then be estimated by employing $\Delta x = \Delta c / (c_{\text{ZnO}} - c_{\text{MgO}})$, where Δc is the x-ray line-width ($\Delta\omega$) for $x=0-0.30$ in the lattice constant unit, and c_{ZnO} and c_{MgO} are the bulk lattice constants.⁴ Using this equation, Δx has been estimated to be 3.78 (angular to linear scale conversion has been done by using the relation $L=R\theta$, where R is the atomic radius of ZnO material of 0.18 nm). Similarly, if we assume that the PL peak energy increases primarily from the compositional fluctuations, then δ can be estimated by^{10,11}

$$\Delta x \cong \Delta E_{\text{PL}} / |E_{\text{ZnO}} - E_{\text{MgO}} - \delta + 2x\delta|, \quad (1)$$

where ΔE_{PL} is the blueshifted energy in $\text{Mg}_x\text{Zn}_{1-x}\text{O}$ alloys for $x=0-0.3$. From this equation, δ has been estimated with to be -4.72 eV; consistent with the upward bowing behavior. In principle, the uncertainty in energy emission measurements is $\Delta E \cong k_{\text{B}}T$, which gives the δ measurement uncertainty of $\Delta\delta \cong 4\Delta E_{\text{PL}} \cong 0.84$ eV. Thus the resultant δ in the $\text{Mg}_x\text{Zn}_{1-x}\text{O}$ alloy for $x=0.3$ should be -4.72 ± 0.84 eV.

The existence of this larger negative bowing, together with the compositional fluctuations, can be described in a first principles approximation by a parabolic model involving

TABLE I. The bowing parameter for the II-O alloys.

| Alloy | Composition (x) | Bandgap bowing δ (eV) | Ref. |
|-------------------------------------|-----------------|------------------------------|----------------|
| Mg _x Zn _{1-x} O | 0–0.30 | –4.86 | This work |
| Mg _x Zn _{1-x} O | 0–1.00 | 0.56 | 8 ^a |
| Mg _x Zn _{1-x} O | 0–0.34 | 1.34 | 8 ^a |
| Be _x Zn _{1-x} O | 0–1.00 | 5.60 | 13 |
| Cd _x Zn _{1-x} O | 0–0.50 | 8.14 | 13 |
| Cd _x Zn _{1-x} O | 0–0.50 | 5.93 | 12 |
| ZnO _{1-x} S _x | 0–0.50 | 3.70 | 14 |
| ZnO _{1-x} Se _x | 0–0.13 | 8.00 | 14 |

^aTheoretical work.

the δ parameter. This speculation satisfies the growth orientation along the c -axis, which is responsible for the spontaneous polarization in the Mg_xZn_{1-x}O/SiC heterointerfaces. Therefore, the alloy polarization can be expressed as a composition-weighted Vegard-like average as $P_{\text{Mg}_x\text{Zn}_{1-x}\text{O}}^{\text{SP}}(x) = xP_{\text{MgO}}^{\text{SP}} + (1-x)P_{\text{ZnO}}^{\text{SP}}$. The δ due to the polarization (P), therefore, can be described by¹¹

$$\delta_{\text{Mg}_x\text{Zn}_{1-x}\text{O}} = 2P_{\text{MgO}} + 2P_{\text{ZnO}} - 4P_{\text{Mg}_{0.5}\text{Zn}_{0.5}\text{O}}. \quad (2)$$

It is noted that the spontaneous polarization for the ZnO and MgO materials has been reported to be -0.050 and -0.070 C/m², respectively.⁹ Substituting these values in Eq. (2), the spontaneous polarization for the Mg_{0.5}Zn_{0.5}O alloys has been estimated to be -0.054 C/m². This value is comparable with the binary ZnO and MgO compounds. It is also expected that this spontaneous polarization in the Mg_xZn_{1-x}O/SiC heterointerface plays an additional role in the negative bandgap bowing.¹² However, for a clearer understanding on this issue, further studies are necessary. Table I shows the δ values for the particular II-O alloys.^{8,13,14}

IV. CONCLUSION

The localized exciton energy of Mg_xZn_{1-x}O alloys deposited on 6H-SiC substrates has been blueshifted in the range 212–248 meV, while the Stokes shift was ~ 30 meV. The large bandgap bowing has been estimated in Mg_xZn_{1-x}O/SiC heterostructure to be -4.72 ± 0.84 eV. This large negative bowing, together with the large Stokes shift, has been attributed to the existence of spontaneous polarization (-0.054 C/m²) due to the polar growth of Mg_xZn_{1-x}O/SiC heterostructure and compositional inhomogeneity locally. These results will contribute to settle down the long standing bandgap bowing nature in the (Mg, Zn, Cd)O matrix.

genuity locally. These results will contribute to settle down the long standing bandgap bowing nature in the (Mg, Zn, Cd)O matrix.

ACKNOWLEDGMENTS

This work is supported by the Australian Research Council.

- ¹U. Ozgur, Y. I. Alivov, V. Liu, M. A. Reshchikov, S. Do, V. Avrutin, S.-J. Cho, and H. Morkoc, *J. Appl. Phys.* **98**, 041301 (2005); A. Ashrafi and C. Jagadish, *ibid.* **102**, 071101 (2007).
- ²S. J. Pearton, D. P. Norton, K. Ip, Y. W. Heo, and T. Steiner, *Prog. Mater. Sci.* **50**, 293 (2005); A. Ashrafi and Y. Segawa, *J. Appl. Phys.* **103**, 093527 (2008); A. B. M. A. Ashrafi, Y. Segawa, K. Shin, and T. Yao, *Phys. Rev. B* **72**, 155302 (2005).
- ³J. F. Sarver, F. L. Katnack, and F. A. Hummel, *J. Electrochem. Soc.* **106**, 960 (1959); S. F. Chichibu, A. Uedono, T. Onuma, B. A. Haskell, A. Chakraborty, T. Koyama, P. T. Fini, S. Keller, S. P. Denbars, J. S. Speck, U. K. Mishra, S. Nakamura, S. Yamaguchi, S. Kamiyama, H. Amano, I. Akasaki, J. Han, and T. Sota, *Nature Mater.* **5**, 810 (2006).
- ⁴A. B. M. A. Ashrafi and Y. Segawa, *J. Vac. Sci. Technol. B* **23**, 2030 (2005).
- ⁵A. F. Wright and J. S. Nelson, *Appl. Phys. Lett.* **66**, 3051 (1995).
- ⁶A. B. M. A. Ashrafi, B.-P. Zhang, N. T. Binh, K. Wakatsuki, and Y. Segawa, *Jpn. J. Appl. Phys., Part 1* **43**, 1114 (2004); A. B. M. A. Ashrafi, N. T. Binh, B.-P. Zhang, and Y. Segawa, *Appl. Phys. Lett.* **84**, 2814 (2004); A. B. M. A. Ashrafi and Y. Segawa, *Appl. Surf. Sci.* **249**, 139 (2005).
- ⁷F. K. Shan, B. I. Kim, G. X. Liu, Z. F. Liu, J. Y. Sohn, W. J. Lee, B. C. Shin, and Y. S. Yu, *J. Appl. Phys.* **95**, 4772 (2004).
- ⁸(a) A. Ohtomo, M. Kawasaki, T. Koida, K. Masubuchi, H. Koinuma, Y. Sakurai, Y. Yoshida, T. Yasuda, and Y. Segawa, *Appl. Phys. Lett.* **72**, 2466 (1998); (b) W. R. L. Lambrecht, S. Limpijumnong, and B. Segal, *Theoretical Studies of ZnO and Related MgZnO Alloy Band Structures* (The Office of Naval Research, Washington, DC, 2005); (c) S. F. Chichibu, A. Tsukazaki, M. Kawasaki, K. Tamura, Y. Segawa, T. Sota, and H. Koinuma, *Appl. Phys. Lett.* **80**, 2860 (2002); (d) Y. Z. Zhu, G. D. Chen, H. Ye, A. Walsh, C. Y. Moon, and S.-H. Wei, *Phys. Rev. B* **77**, 245209 (2008).
- ⁹J. Wu, W. Walukiewicz, K. M. Yu, J. W. Ager III, E. E. Haller, H. Lu, and W. J. Schaff, *Appl. Phys. Lett.* **80**, 4741 (2002); S.-H. Park and D. Ahn, *ibid.* **87**, 253509 (2005).
- ¹⁰L. H. Robins, J. T. Armstrong, R. B. Marinenko, M. D. Vaudin, C. E. Boudlin, J. C. Woicik, A. J. Paul, W. R. Thurber, K. E. Miyano, C. A. Parker, J. C. Roberts, S. M. Bedair, E. L. Piner, M. J. Reed, N. A. Elmasry, S. M. Donovan, and S. J. Pearton, *IEEE International Symposium on Compound Semiconductors*, Monterey, CA, 2000, p. 507.
- ¹¹F. Bernardini and V. Fiorentini, *Phys. Rev. B* **64**, 085207 (2001).
- ¹²T. Makino, Y. Segawa, M. Kawasaki, A. Ohtomo, R. Shiroki, K. Tamura, T. Yasuda, and H. Koinuma, *Appl. Phys. Lett.* **78**, 1237 (2001).
- ¹³(a) S. F. Ding, G. H. Fan, S. T. Li, K. Chen, and B. Xiao, *Physica B* **394**, 127 (2007); (b) T. Gruber, C. Kirchner, R. Kling, F. Reuss, A. Wagg, F. Bertram, D. Forster, J. Christen, and M. Schreck, *Appl. Phys. Lett.* **83**, 3290 (2003).
- ¹⁴(a) N. Fathy and M. Ichimura, *Jpn. J. Appl. Phys., Part 2* **44**, L1295 (2005); (b) Y. Nabetani, T. Mukawa, Y. Ito, T. Kato, and T. Matsumoto, *Appl. Phys. Lett.* **83**, 1148 (2003).